

Implementation and Experimental Validation of a Dual-Loop Digital PID Control System for a Separately Excited DC Motor

Thi Quynh Nhu Truong¹, Thi Hai Yen Tran²

^{1,2} Faculty of Electrical Engineering, Thai Nguyen University of Technology, No. 666, 3/2 Street, Tich Luong Ward, Thai Nguyen Province, Vietnam
Corresponding Author: Thi Hai Yen Tran

ABSTRACT: In the field of industry and automation, digital electric drive systems using DC motors are widely applied due to their high accuracy, wide regulation range, and smooth speed control capability. Nowadays, with the diversity and abundance of electronic components, digital controllers based on microcontrollers are capable of meeting the required performance, while supporting software tools have made programming more convenient. This paper presents the calculation, design, and experimental implementation of a digital control system for a separately excited DC motor using a dual-loop structure, including an inner current feedback loop and an outer speed feedback loop.

In this system, digital PID controllers for both loops are designed based on the modulus optimum criterion to achieve fast dynamic response and improved control performance. The system is simulated and experimentally implemented using MATLAB/Simulink in combination with the Arduino Mega 2560. Experimental results show that the system achieves a small steady-state error (<1%), short settling time, and low overshoot, consistent with theoretical expectations.

These results confirm the effectiveness and feasibility of the proposed control strategy, making it a suitable solution for modern electric drive applications.

Keywords: Digital PID control; Arduino Mega 2560; feedback control; experimental validation; separately excited DC motor

Date of Submission: 05-05-2026

Date of acceptance: 16-05-2026

I. INTRODUCTION

Industrial systems continue to rely heavily on electric drive systems, which play a crucial role in various fields such as manufacturing, automation, and electric transportation [1]. In practice, electric motors exist in many types; however, DC motors in general, and separately excited DC motors in particular, are still widely used due to their outstanding advantages, including flexible speed control characteristics, high starting torque, and relatively simple control structures [2, 3]. Nevertheless, traditional motor drive systems are typically based on analog control, which suffer from several drawbacks such as high sensitivity to noise, susceptibility to temperature variations and component aging, as well as difficulties in system upgrading and expansion [4, 5].

The rapid development of digital control techniques and microprocessor technology has provided an alternative approach. Digital control structures overcome the aforementioned limitations by utilizing programmable processors [6, 7]. The use of digital controllers enables flexible implementation of control algorithms through software, thereby enhancing adaptability and facilitating the modification of control strategies during system operation [8]. Among various control methods, the PID controller remains one of the most fundamental and widely adopted techniques due to its simple structure, high effectiveness, and ease of implementation in both analog and digital systems, which confirms its superiority [9, 10].

For DC motor drive systems, the primary objective of control is to improve system performance. Therefore, the control structure must incorporate appropriate feedback and controllers. The dual-loop control structure, consisting of an inner current loop and an outer speed loop, has been proven to be an optimal solution for enhancing control performance [2,11]. In this configuration, the current loop is responsible for improving transient response and protecting the system against overcurrent conditions, while the speed loop ensures accurate and stable speed regulation [11,12]. When implemented in digital form, the dual-loop structure can achieve superior performance thanks to the flexibility in tuning controller parameters. Moreover, high-speed digital signal processors enable the execution of advanced control algorithms requiring high resolution, fast processing speed, and significant computational capability [7, 8].

In this study, a digital control system for a separately excited DC motor is developed based on a

dual-loop feedback structure, including a negative speed feedback loop and a negative current feedback loop. Digital PID controllers for both loops are designed and implemented on the Arduino Mega 2560 platform, in combination with MATLAB/Simulink for simulation and control algorithm deployment [13,14]. The modulus optimum method is employed to determine the parameters of the digital PID controllers in both loops [15,16]. This method provides an optimal trade-off among performance criteria, including small steady-state error, short settling time, acceptable overshoot (typically below 5%), and sufficient stability margins [15].

The main objective of this paper is to analyze, design, and experimentally validate a digital control system for a separately excited DC motor using a dual-loop feedback structure. The effectiveness of the proposed digital PID controllers is evaluated in terms of performance improvement compared to conventional methods through both MATLAB/Simulink simulations and experimental implementation on the Arduino Mega 2560 platform.

The remainder of this paper is organized as follows. Section 2 describes the system and its modeling. Section 3 details the controller design. Section 4 presents the experimental results. Section 5 provides the conclusions.

II. SYSTEM DESCRIPTION AND MODELING

The performance of the speed control system for a separately excited DC motor is directly evaluated based on experimental results using a digital controller. The experimental system is configured with the following main components:

- **AC–DC Converter:** A three-phase fully controlled bridge rectifier using thyristors is employed to convert AC voltage into DC voltage supplying the armature of the motor. The output voltage can be adjusted via the firing angle, thereby enabling indirect control of the motor speed.

- **Separately Excited DC Motor** (Fig 2. 1): This motor serves as the main controlled plant. The field winding is supplied independently to maintain a constant magnetic flux, which simplifies the control model and enhances speed regulation capability. The motor specifications are as follows: rated power $P = 2.6$ kW, rated speed $n = 1450$ rpm, rated armature and field voltage $U_u = U_f = 115$ V, rated current $I = 22.5$ A, armature resistance $R_u = 0.27$ Ω , armature inductance $L_u = 0.14$ H, and moment of inertia $GD^2 = 0,127$ [kg.m²].



Fig 2. 1. The experimental setup consists of a dc motor, a generator, and a tachogenerator.

- **Generator Load:** The generator is mechanically coupled to the motor shaft to provide a variable mechanical load, enabling the evaluation of system performance under different loading conditions. The generator specifications are as follows: power range $P = 0.02$ – 1.35 kW, rated speed range $n = 20$ – 1450 rpm, rated voltage range $U = 27$ – 220 V, field voltage $U_f = 330$ V, rated current $I = 22.5$ A, armature resistance $R_a = 3.65$ Ω , armature inductance $L_a = 0.125$ H, and moment of inertia $GD^2 = 0,0076$ [kg.m²]

- **Tachogenerator:** The tachogenerator is used to measure the rotational speed of the motor and generate a feedback signal for the speed control loop.

- **Digital Controller:** The system employs an Arduino Mega 2560 in combination with MATLAB/Simulink to implement the digital PID control algorithm. The control signals are computed in the digital domain and then applied to control the power converter.

Based on the above hardware configuration, the electric drive system is organized using a cascaded dual-loop control structure, consisting of:

- **Inner Current Loop:** This is the inner control loop, responsible for fast regulation of the armature current. It improves transient response and provides protection against overcurrent conditions. Due to its faster dynamics compared to the speed loop, the current loop ensures rapid system response. In this loop, the measured

current is compared with the reference current, and the error signal is processed by the current controller R_i to generate the control signal for the power converter.

Outer Speed Loop: This is the outer control loop, which regulates the motor speed according to the reference value, ensuring small steady-state error and high stability. The speed feedback signal from the tachogenerator is compared with the reference speed, and the resulting error is processed by the speed controller R_n to generate the current reference for the inner loop.

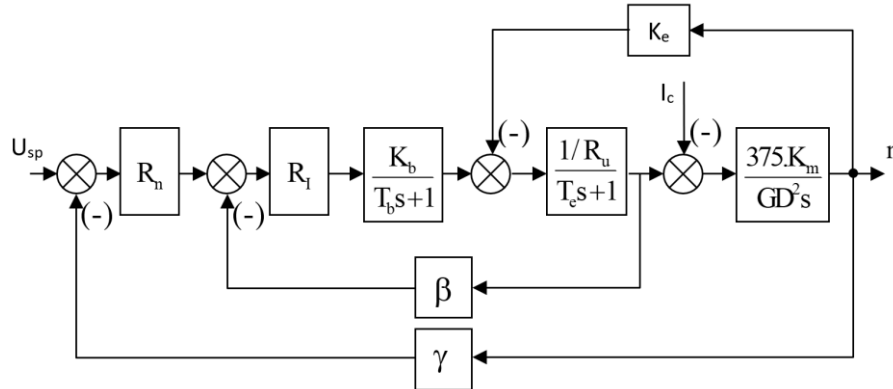


Fig 2. 2. Block diagram of the dual-loop speed control system for a separately excited DC motor with negative speed and current feedback

Where K_b and T_b denote the gain and time constant of the AC–DC converter, respectively; R_u is the armature resistance of the motor; $T_u = \frac{L_u}{R_u}$ is the electrical time constant of the motor, representing the dynamic behavior of the armature circuit; K_e is the back electromotive force constant, with $K_e = \frac{1}{K_D}$, and the torque constant is given by $K_M = 9.55K_e$; $T_m = \frac{GD^2 R_u}{375K_M K_e}$ is the electromechanical time constant of the motor.

In addition, the feedback-related parameters, including the speed feedback coefficient γ , the current feedback coefficient β , and the load current I_c , are used for signal normalization and regulation within the control system.

With the dual-loop control structure consisting of a current feedback loop and a speed feedback loop, as illustrated in Fig 2. 2, the control tasks are effectively decoupled into fast dynamics (current loop) and slow dynamics (speed loop). This structure enhances overall control performance, improves disturbance rejection capability, and ensures system stability.

III. CONTROLLER DESIGN

In this study, within the dual-loop control structure, the controllers associated with each feedback loop are designed according to the modulus optimum criterion to ensure fast dynamic response and improved transient performance.

The desired optimal transfer function is defined as:
$$W_c = \frac{1}{2\tau^2 s^2 + 2\tau s + 1} \tag{1}$$

In the controller design for the current and speed loops, the parameter τ in (1) is specified as τ_i , và τ_n

3.1. Current Controller Design

Assumptions and Model Simplification: In the design of the current control loop, the back electromotive force (EMF) of the motor, $E = K_e n$, is assumed to be constant over a short time interval. This assumption is justified because the mechanical time constant is significantly larger than the electrical time constant, and the speed varies much more slowly than the armature current. Therefore, the effect of the back EMF can be neglected in the design of the current control loop. Based on the overall system structure, the current control loop can be represented as shown in Fig 3. 1:

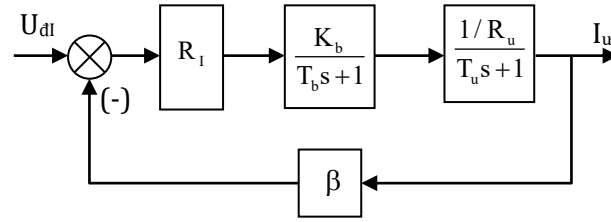


Fig 3. 1. Block diagram of the current control loop considered independently.

To determine R_I , the modulus optimum method is applied, yielding R_I as given in (2)

$$W_{kl}(s) = \frac{R_I(s)W_o(s)}{1 + R_I(s)W_o(s)} \Rightarrow R_I(s) = \frac{W_{kl}(s)}{[1 - W_{kl}(s)]W_o(s)} \quad (2)$$

Where:

$$W_o = \frac{\beta K_b}{R_u(T_b s + 1)(T_u s + 1)} \quad (3)$$

According to the modulus optimum criterion, the controller parameters are selected based on a trade-off between response speed and system stability. The following condition must be satisfied: $T_b < T_u < \frac{t_p}{6}$, where T_b is the time constant of the converter, T_u is the electrical time constant of the motor, and t_p is the desired settling time.

The current controller R_I is calculated as follows:

$$R_I(s) = \frac{W_c(s)}{[1 - W_c(s)]W_o(s)} = \frac{1}{2\tau_i s(1 + \tau_i s)W_o(s)} = \frac{R_u(T_b s + 1)(T_u s + 1)}{\beta K_b 2\tau_i s(1 + \tau_i s)} \quad (4)$$

Based on the actual system parameters, after calculation and according to the selection principle of the time constant τ_i in the optimal transfer function of the current loop under the modulus optimum criterion, τ_i is chosen as $\tau_i = T_b = 0,00167$ (s). Therefore, equation(4) can be rewritten as follows:

$$R_I(s) = \frac{R_u(T_u s + 1)}{2\beta K_b T_b s} = K_I \frac{1 + T_u s}{s} = \frac{K_I}{s} + K_I T_u = \frac{K_I}{s} + K_p \quad (5)$$

In the continuous-time domain, the controller is described by the following relation:

$$U_{dk}(s) = K_p \left(1 + \frac{1}{T_i s} \right) U_{vi}(s) \quad (6)$$

After discretization, the control law of the current controller can be expressed in the form of a difference equation:

$$R_I(z) = Z[R_I(s)] = Z \left[\frac{K_I}{s} + K_p \right] = \left[\frac{K_I z}{z-1} + K_p \right] = \frac{U_{dk}(z)}{U_{dkn}(z)} \quad (7)$$

$$U_{dk}(z) = (z^{-1})U_{dk}(z) + (K_I + K_p)U_{dkn}(z) - K_p z^{-1}U_{dkn}(z) \quad (8)$$

$$u_{dk}[k] = u_{dk}[k-1] + (K_I + K_p)u_{dkn}[k] - K_p u_{dkn}[k-1] \quad (9)$$

3.2. Speed Controller Design

The design principle of the speed controller is established after the current control loop has been designed, with the mathematical model of the current loop given as follows: $W_{tu} = \frac{1}{2T_b^2 s^2 + 2T_b s + 1}$ (10)

Therefore, the structure of the speed control loop can be represented as shown in Fig 3. 2.

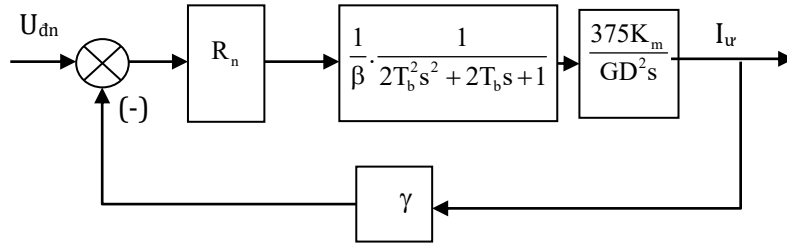


Fig 3. 2. Block diagram of the speed control loop based on the completed current control loop.

The mathematical description of the system corresponding to Fig 3. 2. is given by equations(11)(12):

$$W_{kn}(s) = \frac{R_n(s)W_{on}(s)}{1 + R_n(s)W_{on}(s)} \Rightarrow R_n(s) = \frac{W_{kn}(s)}{[1 - W_{kn}(s)]W_{on}(s)} \quad (11)$$

Where:

$$W_{on}(s) = \frac{375K_m}{\beta(2T_b^2 s^2 + 2T_b s + 1)GD^2 s} \quad (12)$$

According to the modulus optimum criterion for the speed control loop, the time constant is chosen as $T = 2T_b$

$$R_n(s) = \frac{W_c(s)}{[1 - W_c(s)]W_{on}(s)} = \frac{1}{2\tau_n s(1 + \tau_n s)W_{on}(s)} = \frac{\beta GD^2 (2T_b^2 s^2 + 2T_b s + 1)s}{\gamma 375K_m 2\tau_n s(1 + \tau_n s)} \quad (13)$$

Since $2T_b^2 < 0,001$ this term can be neglected in the calculation. Hence:

$$R_n(s) = \frac{\beta GD^2 (2T_b s + 1)s}{\gamma 375K_m 2\tau_n s(1 + \tau_n s)} = \frac{\beta GD^2}{\gamma 375K_m 4T_b} = K_p \quad (14)$$

For the actual system, since $2T_b < t_p/6$ the time constant is selected as $\tau_n = 2T_b$.

Thus, the speed controller is selected as a proportional (P) controller. By discretizing (14) the control law of the speed controller can be expressed in the form of a difference equation as given in (15):

$$R_n(z) = Z[R_n(s)] = Z[K_p] = \frac{U_{dkn}(z)}{U_v(z)} \quad (15)$$

where $U_{dkn}(z) = K_p U_v(z)$; $U_{dkn}[k] = K_p U_v[k]$

IV. EXPERIMENTAL RESULTS

In this study and experimental implementation, the controller design is carried out using MATLAB/Simulink. The current controller parameters are configured in the *Current Controller* block, while the speed controller parameters are set in the *Speed Controller* block. The designed control algorithm is then deployed onto the Arduino Mega 2560 microcontroller.

Fig 4. 1 illustrates the speed and current responses under no-load and varying load conditions. Under no-load operation at 200 rpm, the system demonstrates fast tracking performance with a settling time of approximately 0.5 s and a negligible steady-state error ($S_t < 1\%$). When the reference speed changes from 200 rpm to 400 rpm, the response remains fast with good tracking capability and a small overshoot of about 3–5%, indicating good dynamic performance.

Under load disturbances (Load 1 and Load 2), the speed deviates but is quickly restored, demonstrating effective disturbance rejection capability. The armature current increases accordingly to compensate for the load torque, confirming effective coordination between the inner and outer control loops. When the load is removed, a small transient overshoot (approximately 5%) is observed, followed by rapid stabilization.

These results are consistent with the modulus optimum design, which theoretically ensures fast response, acceptable overshoot, and small steady-state error. Therefore, the experimental results confirm that the proposed dual-loop digital control system achieves performance close to the theoretical expectations

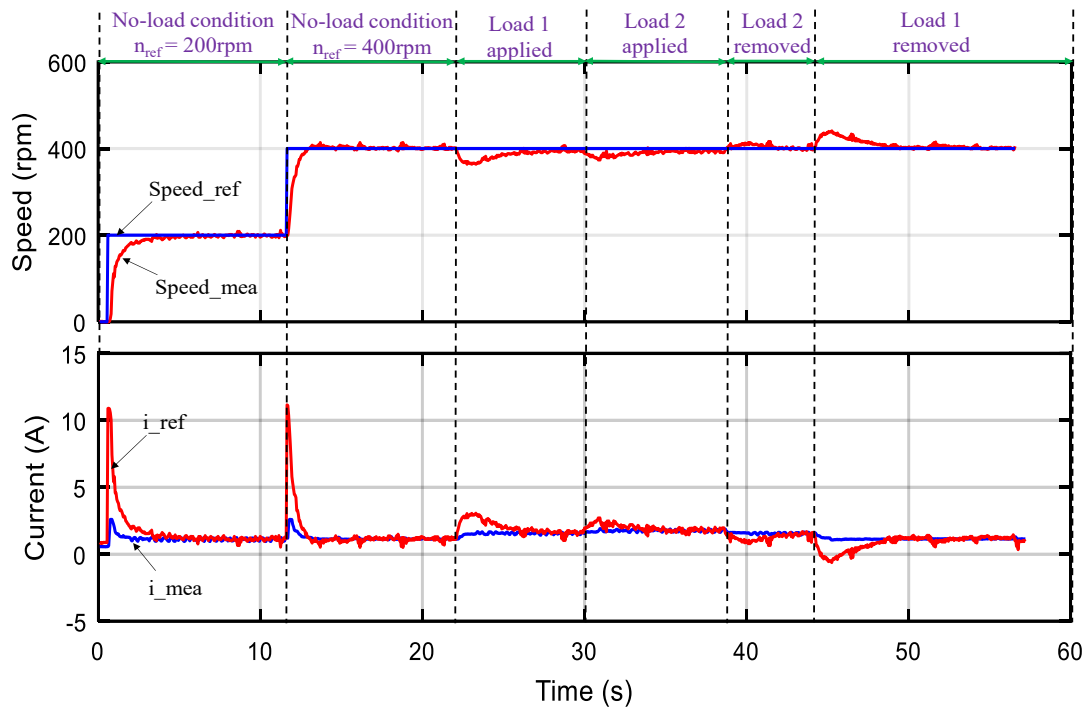


Fig 4. 1. Speed and current responses of the system under no-load and load conditions.

V. CONCLUSION

This paper presents the design and experimental implementation of a separately excited DC motor drive system using a dual-loop control structure, consisting of an inner current loop and an outer speed control loop. The proposed approach employs digital PID controllers implemented using MATLAB and the Arduino Mega 2560 platform, providing a flexible solution for adjusting controller parameters and demonstrating effectiveness for modern electric drive systems.

The controller parameters are designed based on the modulus optimum criterion, ensuring fast dynamic response and stable system performance. By separating the control tasks into two loops, the inner current loop enhances transient response and provides disturbance rejection capability, while the outer speed loop ensures accurate speed tracking with minimal steady-state error.

Experimental results show that the proposed system satisfies the required performance criteria, including small steady-state error, short settling time, and stable operation under varying load conditions. The digital implementation also demonstrates clear advantages over conventional analog control methods in terms of flexibility, ease of tuning, and scalability.

However, some limitations remain, such as the limited computational capability of low-cost microcontrollers and the reliance on classical PID control, which may not be optimal under highly nonlinear or uncertain conditions. Future work will focus on improving control performance by applying advanced control strategies, such as adaptive control, robust control, or intelligent control methods. In addition, the proposed framework can be extended to more complex drive systems, such as multi-phase machines or field-oriented control (FOC) of AC motors.

ACKNOWLEDGEMENT

This research was supported by a university research grant from Thai Nguyen University of Technology (TNUT). We thank our colleagues at TNUT for their valuable insights and expertise that greatly assisted this research

REFERENCES

- [1]. R. Krishnan, *Electric Motor Drives: Modeling, Analysis, and Control*. Prentice Hall, 2001.
- [2]. W. Leonhard, *Control of Electrical Drives*, 3rd ed. Springer, 2001.
- [3]. S. N. Vukosavić, *Digital Control of Electrical Drives*. Springer, 2007.
- [4]. B. C. Kuo, *Digital Control Systems*, 2nd ed. Oxford University Press, 1995.
- [5]. K. Ogata, *Modern Control Engineering*, 5th ed. Prentice Hall, 2010.
- [6]. T. M. Jahns and V. Blasko, "Recent advances in power electronics and motor drives," *IEEE Trans. Power Electron.*, vol. 16, no. 1, pp. 1–11, 2001.
- [7]. A. Emadi, *Handbook of Automotive Power Electronics and Motor Drives*. CRC Press, 2005.

- [8]. G. F. Franklin, J. D. Powell, and M. L. Workman, *Digital Control of Dynamic Systems*, 3rd ed. Addison-Wesley, 1998.
- [9]. K. J. Åström and T. Hägglund, *PID Controllers: Theory, Design, and Tuning*, 2nd ed. ISA, 1995.
- [10]. K. J. Åström and T. Hägglund, "The future of PID control," *Control Eng. Pract.*, vol. 9, no. 11, pp. 1163–1175, 2001.
- [11]. R. D. Doncker, D. W. J. Pulle, and A. Veltman, *Advanced Electrical Drives: Analysis, Modeling, Control*. Springer, 2011.
- [12]. M. P. Kazmierkowski and H. Tunia, *Automatic Control of Converter-Fed Drives*. Elsevier, 1994.
- [13]. MATLAB/Simulink, *User's Guide*. The MathWorks Inc., 2023.
- [14]. Arduino, *Arduino Mega 2560 Reference Design*. Arduino LLC, 2023.
- [15]. C. Kessler, "Das symmetrische Optimum," *Regelungstechnik*, vol. 6, no. 1, pp. 395–400, 1958.
- [16]. S. Preitl and R. E. Precup, "An extension of tuning relations after symmetrical optimum method for PI and PID controllers," *Automatica*, vol. 35, no. 10, pp. 1731–1736, 1999.